Collective excitations of a hot QCD medium in a time dependent background magnetic field

Gowthama K K[*] and Vinod Chandra[†]

Indian Institute of Technology Gandhinagar, Gandhinagar-382355, Gujarat, India

Collective modes within a hot quantum chromodynamics (QCD) medium are obtained from the polarization tensor, considering both constant and time-varying electromagnetic fields. In both scenarios, five complex modes emerge, reliant on the wave vector (k), with electrical conductivity exerting significant influence. The impact of the modes on the energy loss of heavy quarks in the hot QCD medium with a background electromagnetic field has been studied by obtaining the induced electric field in terms of the polarization tensor while invoking Wong's equations. The findings are seen to be consistent with analogous approaches, reinforcing the significance of the results.

I. INTRODUCTION

The Relativistic Heavy Ion Collider (RHIC) and the Large Hadron Collider (LHC) have conducted heavy-ion experiments, providing evidence of the existence of an intriguing form of matter known as quark-gluon plasma (QGP) [1]. This unique state of matter arises from the intense interactions of quarks and gluons as dictated by the underlying theory of strong interaction force; viz., quantum chromodynamics (QCD) exists for very short times (a few fm/c) at exceedingly high temperatures. Given the complex nature of the strong interaction and, hence, the QGP, its direct investigation proves challenging, necessitating indirect methods to unravel its properties. Among these, two prominent signatures are jet quenching and collective flow, which have been observed at the RHIC and the LHC. Through these experiments, compelling evidence has emerged substantiating the presence of the QGP and its strong coupling nature that is exemplified by the observation of an extremely low shear viscosity to entropy density ratio, further supporting the notion of the QGP as a near-ideal fluid [2,3].

Experiments at the RHIC and the LHC observed enhanced directed flow of D/D^0, indicating the presence of a strong initial magnetic field in heavy-ion collisions [4,5]. The produced magnetic field decays slowly in the medium and may persist for a longer time due to the backreaction

---
[*]k_gowthama@iitgn.ac.in
[†]vchandra@iitgn.ac.in

from the medium. The behavior of the magnetic field in the medium depends on the conductivity of the medium [6–10]. The behavior of the QGP medium may depend on the persistent field, and hence it is vital to study the response of the medium to such a field. Numerous studies delve into this, encompassing electrical conductivity in weak and time dependent electromagnetic fields [11–21], as well as thermal and thermoelectric responses of the medium [22–25].

The investigation of the QGP necessitates an in-depth exploration of its collective excitations, which carry crucial information into both equilibrated and evolving non(near)-equilibrated QGP. In this context, it is imperative to examine both quark and gluonic collective modes within the QGP medium. The collective modes of the QGP medium have been studied through the linear response formalism [26,27], with momentum anisotropy [28–30], with equation of state effects [31,32].

The magnetic field in the early stages of the collision is argued to be of the order $|qB| \sim 10–15m_\pi^2$ [33–36], which is much larger than the temperature, i.e. $qB \gg T^2$. In this regime, the system obeys Landau quantization, and the fermion dynamics can be treated under the lowest Landau level approximation [37,38]. As the magnetic field rapidly decays, the temperature becomes the dominant scale, $qB \ll T^2$. The fermions undergo cyclotron motion due to the presence of the magnetic field. The analysis of the collective modes in the weak field limit has been studied through the perturbative QCD methods [37,39,40] and the linear response theory [41]. The linear response theory and perturbative QCD results are generally seen to match qualitatively, especially at higher temperatures.

In this study, we focus on comprehending the collective excitations of the QGP medium in the presence of a weak, time-varying magnetic field through the polarization tensor.

This marks a novel attempt to understand the properties of the hot QCD medium under the influence of time dependent magnetic fields, with the inclusion of electric (σ_e) and Hall (σ_H) conductivities obtained through the linear response theory approach. Our analysis unfolds the presence of two complex modes and three purely imaginary modes, two of which display positive growth, signifying potential instabilities within the medium.

Heavy quarks/antiquarks, produced in the early stages of collisions, offer valuable insights into the entire spacetime evolution of the QGP medium, making them excellent probes of the medium. The energy loss of heavy quarks has been studied through the transport theory approach [42–46] and within the finite temperature field theory approach [47–49]. Our focus here is on studying how bottom and charm quarks lose energy while traversing an isotropic, collisional QGP. We model the collisions employing the relaxation-time approximation (RTA) collisional kernel within the Boltzmann transport equation. When a charged quark moves through the hot QCD medium, it induces an electric field, which, in turn, generates a Lorentz force back on the quark, causing it to lose energy. The induced electric field is obtained by solving Maxwell's equation with the polarization tensor obtained through the transport theory. The induced field is employed in Wong's equation to study the energy loss of the heavy quarks.

The paper is organized as follows: Sec. II deals with the basic formalism of the polarization tensor with the consideration of different cases of the magnetic field. In Sec. III, the brief mathematical formalisms for the polarization tensor and the different collective modes are presented in different subsections. The formalism for the energy loss of heavy quarks has been presented in Sec. IV. Section V contains the results and discussion, and Sec. VI offers a summary and conclusions of the present work.

Notations and conventions. The subscript k denotes the particle species. The quantity q_k is the electric charge of the kth species. The particle velocity is defined as $\mathbf{v} = \frac{\mathbf{p}}{\epsilon}$, where $\mathbf{p}$ is the momentum and $\epsilon = \sqrt{p^2 + m_f^2}$ is the energy (with m_f as the mass of quark with flavor f) of the particle. The component of a three vector $\mathbf{A}$ is denoted with the Latin indices A^i. The quantities $E = |\mathbf{E}|$ and $B = |\mathbf{B}|$ denote the magnitudes of the electric and magnetic fields.

II. POLARIZATION TENSOR IN HOT QCD MEDIUM IN ELECTROMAGNETIC FIELDS

The propagator of the hot QCD medium can be obtained from the polarization tensor, invoking Maxwell's equation. The polarization tensor is related to the induced current in the medium due to the external electromagnetic field. In this work, we adopt the transport theory approach while employing the RTA for the collisional kernel.

We consider the transport equation with $F^{\mu\nu}$, the external electromagnetic field tensor,

$$v^\mu \partial_\mu \delta f_k + q_k v_\mu F^{\mu\nu} \partial_\nu^{(p)} f_k = -\frac{\delta f_k}{\tau_R}, \quad (1)$$

with q_k being the charge of the particle and f_k being the quarks/antiquarks momentum distribution function;

$$f_k = f_k^0 + \delta f_k, \qquad f_k^0 = \frac{1}{1 + \exp(\beta(\epsilon_k \mp \mu))}, \quad (2)$$

with f_k^0 being the near equilibrium distribution function. The collision term has been chosen to be the RTA kernel, with τ_R being the relaxation time [50].

The general form of the induced vector current in the QCD medium with a nonvanishing quark chemical potential μ in terms of quark and antiquark momentum distribution function $f_k = f_k^0 + \delta f_k$ is as follows:

$$\mathbf{j} = 2N_c \sum_f \int dP\, \mathbf{v} (q_q f_q - q_{\bar{q}} f_{\bar{q}}), \quad (3)$$

where v_i is the component of velocity and $dP = \frac{d^3\mathbf{p}}{(2\pi)^3}$. The flavor summation (over the up, down, and strange quarks) arises from the degeneracy factor $2N_c \sum_f$ of the quarks/antiquarks with N_c number of colors. The electric current can be written as

$$j^i = \sigma_e \delta^{ij} E_j + \sigma_H \epsilon^{ij} E_j, \qu(4)$$

where σ_e and σ_H are the Ohmic and Hall conductivities, respectively. The conductivities can be obtained by solving the transport equation with the nonequilibrium part of the distribution function $\delta f_k = (\mathbf{p}.\mathbf{\Xi}) \frac{\partial f_k^0}{\partial \epsilon_k}$, containing the electric and magnetic fields. The vector $\mathbf{\Xi}$ is related to the strength of the electromagnetic field and its first-order (leading-order) spacetime derivatives, with the following form:

$$\mathbf{\Xi} = \alpha_1 \mathbf{E} + \alpha_2 \dot{\mathbf{E}} + \alpha_3 (\mathbf{E} \times \mathbf{B}) + \alpha_4 (\dot{\mathbf{E}} \times \mathbf{B}) + \alpha_5 (\mathbf{E} \times \dot{\mathbf{B}})$$
$$+ \alpha_6 (\mathbf{\nabla} \times \mathbf{E}) + \alpha_7 \mathbf{B} + \alpha_8 \dot{\mathbf{B}} + \alpha_9 (\mathbf{\nabla} \times \mathbf{B}). \quad (5)$$

Here, α_i [$i = (1, 2, \ldots, 9)$] are the unknown functions that relate to the respective electric charge transport coefficients and can be obtained by the microscopic description of the QCD medium. The coefficients are found, as derived in Ref. [21], to be

$$\alpha_1 = -\frac{\tilde{\Omega}_k}{2} (I_1 e^{\eta_1} + I_2 e^{\eta_2}), \qu(6)$$

$$\alpha_3 = \frac{q_{fk} i}{2\epsilon} (I_1 e^{\eta_1} - I_2 e^{\eta_2}), \qu(7)$$

$$\alpha_5 = -\frac{\tau_R q_{fk} i}{2\epsilon} (I_1 e^{\eta_1} - I_2 e^{\eta_2}), \qu(8)$$

$$\alpha_2 = \frac{\left(\frac{\tilde{\Omega}_k \tau_R}{2} + \frac{i\Omega_k^2 \tau_R^2}{2}\right) I_1 e^{\eta_1} + \left(\frac{\tilde{\Omega}_k \tau_R}{2} - \frac{i\Omega_k^2 \tau_R^2}{2}\right) I_2 e^{\eta_2}}{1 + \Omega_k^2 \tau_R^2}, \quad (9)$$

$$\alpha_4 = \frac{-\left(\frac{\tilde{\Omega}_k^2 \tau_R^2}{2F} + \frac{iq_{fk}\tau_R}{2\epsilon}\right) I_1 e^{\eta_1} - \left(\frac{\tilde{\Omega}_k^2 \tau_R^2}{2F} - \frac{iq_{fk}\tau_R}{2\epsilon}\right) I_2 e^{\eta_2}}{1 + \Omega_k^2 \tau_R^2}, \quad (10)$$

with $\Omega_k = \frac{q_{fk}B}{\epsilon}$ represents the cyclotron frequency at finite B and $\tilde{\Omega}_k = \frac{q_{fk}F}{\epsilon}$, where $F = \sqrt{B(B - \tau_R \dot{B})}$ for the time-varying magnetic field. Here the terms η_j and I_j are defined as

$$\eta_j = -\frac{t}{\tau_R} + a_j \frac{q_{f_k} i}{\epsilon} \int F dt, \qquad I_j = \int \frac{e^{-\eta_j}}{F}, \quad (11)$$

with $a_1 = 1$ and $a_2 = -1$. Now, we solve the master equation of α_i for various choices of the electromagnetic fields **E** and **B**.

A. Case I: Constant electric and magnetic fields

For the case of constant electric and magnetic fields, the terms α_2, α_4, α_5 disappear, and the coefficients α_1 and α_3 correspond to the Ohmic and Hall conductivity, respectively, as described in Ref. [20]. The expression for α_1 and α_3 are given by

$$\alpha_1 = \frac{-\epsilon q_{f_k}}{\tau_R \left[\left(\frac{\epsilon}{\tau_R}\right)^2 + (q_{f_k}B)^2\right]}, \qquad \alpha_3 = \frac{-q_{f_k}^2}{\left[\left(\frac{\epsilon}{\tau_R}\right)^2 + (q_{f_k}B)^2\right]}. \quad (12)$$

Employing Eq. (12) in Eq. (3), we obtain $j^i = \sigma_e \delta^{ij} E_j + \sigma_H \epsilon^{ij} E_j$ with σ_e and σ_H denoting the electrical and Hall conductivities, respectively. The results obtained are in agreement with the observations of Ref. [11]. The chemical potential plays an important role with the Hall conductivity vanishing at $\mu = 0$, zero chemical potential. The electric current is written as

$$j_e = \frac{E(t)}{3} 2N_c \sum_k \sum_f (q_{f_k})^2 \int \frac{d^3\mathbf{p}}{(2\pi)^3} p^2 \left(-\frac{\partial f_k^0}{\partial \epsilon}\right)$$
$$\times \frac{1}{\tau_R \left[\left(\frac{\epsilon}{\tau_R}\right)^2 + (q_{f_k}B)^2\right]}, \quad (13)$$

$$j_H = \frac{E(t)}{3} 2N_c \sum_k \sum_f (q_{f_k})^2 \int \frac{d^3\mathbf{p}}{(2\pi)^3} \frac{p^2}{\epsilon} \left(-\frac{\partial f_k^0}{\partial \epsilon}\right)$$
$$\times \frac{q_{f_k}B}{\left[\left(\frac{\epsilon}{\tau_R}\right)^2 + (q_{f_k}B)^2\right]}, \quad (14)$$

which agrees with the results of [51]. The transverse component, σ_H, vanishes in the presence of a strong

magnetic field due to the $1 + 1 - D$ Landau dynamic, with the longitudinal electrical conductivity being the dominant electrical charge transport.

B. Case II: Response to time-varying electromagnetic field

In the case of time dependent electric and magnetic fields, we choose a particular magnetic field of the form $\mathbf{B} = B_0 e^{-\frac{t}{\tau_B}}\hat{\mathbf{z}}$, where B_0 is its amplitude and τ_B is the decay time parameter [52,53] such that $F = B\sqrt{1 + \frac{\tau_R}{\tau_B}}$. This form of **B** may depict the rapidly decaying magnetic field in noncentral heavy-ion collisions. The decay rate will depend on the medium properties and is governed by τ_B (can be treated as a phenomenological parameter). With the assumption that the cyclotron frequency Ω_k is approximately equal to the decay frequency (τ_B^{-1}) of the magnetic field, Eq. (11) reduces to the following form:

$$\eta_j = -\frac{t}{\tau_R} + a_j \left(i\frac{\sqrt{1 + \frac{\tau_R}{\tau_B}}}{\tau_B} t\right), \quad (15)$$

$$I_j = \frac{1}{\sqrt{1 + \frac{\tau_R}{\tau_B}} B_0} \frac{e^{\left(\frac{1}{\tau_R} + \frac{1}{\tau_B} - a_j i \frac{\sqrt{1 + \frac{\tau_R}{\tau_B}}}{\tau_B}\right) t}}{\left(\frac{1}{\tau_R} + \frac{1}{\tau_B} - a_j i \frac{\sqrt{1 + \frac{\tau_R}{\tau_B}}}{\tau_B}\right)}, \quad (16)$$

and we proceed with the estimation of all α_i coefficients by substituting Eqs. (15) and (16) in Eqs. (6)–(10). Incorporating the nonzero contributions associated with $\alpha_i (i = 1, 2, …, 5)$ in Eq. (5), we obtain five components of the induced current $\mathbf{j} = j_e \hat{\mathbf{e}} + j_H (\hat{\mathbf{e}} \times \hat{\mathbf{b}})$ as follows:

$$j_e = j_e^{(0)} + j_e^{(1)}, \qquad j_H = j_H^{(0)} + j_H^{(1)} + j_H^{(2)}, \quad (17)$$

where j_e corresponds to the electric current in the direction of the electric field $\hat{\mathbf{e}}$ and j_H is the electrical current in the direction perpendicular to both electric and magnetic fields $(\hat{\mathbf{e}} \times \hat{\mathbf{b}})$ with

$$j_e^{(0)} = \frac{2E}{3} N_c \sum_k \sum_f (q_{fk})^2 \int dP \frac{p^2}{\epsilon^2} \left(-\frac{\partial f_k^0}{\partial \epsilon}\right) M_1, \quad (18)$$

$$j_e^{(1)} = \frac{2\dot{E}}{3} N_c \sum_k \sum_f (q_{fk})^2 \int dP \frac{p^2}{\epsilon^2} \frac{\partial f_k^0}{\partial \epsilon} M_2, \quad (19)$$

$$j_H^{(0)} = \frac{2E}{3} N_c \sum_k \sum_f (q_{fk})^3 \int dP \frac{p^2}{\epsilon^3} \left(-\frac{\partial f_k^0}{\partial \epsilon}\right) M, \quad (20)$$

$$j_H^{(1)} = \frac{2\dot{E}}{3} N_c \sum_k \sum_f (q_{fk})^3 \int dP \frac{p^2}{\epsilon^3} \frac{\partial f_k^0}{\partial \epsilon} M_3, \quad (21)$$

$$j_H^{(2)} = \frac{2E}{3\tau_B} N_c \sum_k \sum_f (q_{fk})^3 \int dP \frac{p^2}{\epsilon^3} \left(-\frac{\partial f_k^0}{\partial \epsilon}\right) \tau_R M, \quad (22)$$

where $\dot{E} = |\dot{\mathbf{E}}|$ and M_j $(j = 1, 2, 3)$ functions can be defined as $M_1 = (\frac{1}{\tau_R} + \frac{1}{\tau_B})M$, $M_2 = -(\tau_R M_1 - \frac{\tau_R^2}{\tau_B^2}M)/(1 + (\frac{\tau_R}{\tau_B})^2)$, and $M_3 = (\tau_R M + \tau_R^2 M_1)/(1 + (\frac{\tau_R}{\tau_B})^2)$ with

$$M = \left[\frac{1}{\tau_R} + \frac{1}{\tau_B} + \frac{\sqrt{1 + \frac{\tau_R}{\tau_B}}}{\tau_B}\right]^{-1}. \quad (23)$$

In Eqs. (18)–(22), the leading-order Ohmic current is represented by $j_e^{(0)}$, while $j_e^{(1)}$ signifies the correction due to the Ohmic current resulting from the time-varying nature of the fields. The Hall current in the medium, produced by perpendicular electric and magnetic fields, is denoted by $j_H^{(0)}$, while its corrections from $(\dot{\mathbf{E}} \times \mathbf{B})$ and $(\mathbf{E} \times \dot{\mathbf{B}})$ are represented by $j_H^{(1)}$ and $j_H^{(2)}$, respectively.

From these expressions for the induced current, the polarization tensor can be obtained using $\Pi^{\mu\nu} = \frac{\delta j_{ind}^\mu}{\delta A_\nu}$ in the temporal gauge with $A_0 = 0$ and $A^i = \frac{E^i}{i\omega}$,

$$\Pi^{ij} = i\omega\sigma_e\delta^{ij} + i\omega\sigma_H\epsilon^{ij}. \quad (24)$$

The Fourier transformed Maxwell equation is

$$-ik_\nu F^{\mu\nu}(K) = J_{ind}^\mu(K) + J_{ext}^\mu(K), \quad (25)$$

where $J_{ext}^\mu(K)$ is the external current. The induced current can be expressed in terms of the polarization tensor, written as

$$J_{ind}^\mu(K) = \Pi^{\mu\nu}(K)A_\nu. \quad (26)$$

The Maxwell equation can be written as

$$\left[K^2 g^{\mu\nu} - k^\mu k^\nu + \Pi^{\mu\nu}\right]A_\nu(K) = J_{ext}^\mu(K). \quad (27)$$

Considering the temporal gauge $A_0 = 0$, writing the equation in terms of the electric field,

$$[\Delta^{ij}(k)]^{-1}E_j = i\omega J_{ext}^i, \quad (28)$$

where

$$\left[\Delta^{ij}(k)\right]^{-1} = \left[(k^2 - \omega^2)\delta^{ij} - k^i k^j + \Pi^{ij}(k)\right] \quad (29)$$

is the inverse of the propagator. The poles of the propagator, $[\Delta^{ij}(k)]$, give us the dispersion relation of the collective modes.

III. COLLECTIVE MODES: FINDING THE POLES OF THE PROPAGATOR

A. Decomposition of polarization tensor

The polarization tensor encodes the interaction of the medium. Hence, the properties of the QGP medium can be analyzed by studying the structure of the polarization tensor. The general structure of the polarization tensor in a magnetic field has been studied in Ref. [37].

We have obtained the form of the polarization tensor through the semiclassical transport theory approach in Eq. (24). The polarization tensor in the isotropic medium can be expanded in terms of two components. The longitudinal component $P_L^{ij} = k^i k^j / k^2$, and the transverse component $P_T^{ij} = \delta^{ij} - k^i k^j / k^2$. The background magnetic field induces anisotropy in the medium, and hence an additional two components are required to describe the polarization tensor in the presence of a magnetic field, $P_b^{ij} = b^i b^j$ and $P_{bk}^{ij} = \epsilon^{ij\eta} b_\eta$, where $b^i = B^i / |B|$ is the unit vector along the magnetic field and is taken to be such that $b^i k_i = 0$. With this, the polarization tensor can be expanded as

$$\Pi^{ij} = \alpha_0 P_L^{ij} + \beta_0 P_T^{ij} + \gamma_0 P_b^{ij} + \delta_0 P_{bk}^{ij}, \quad (30)$$

where $\alpha, \beta, \gamma, \delta$ are the scalar structure constants. These can be obtained by taking the appropriate projections of the polarization tensor with the following projections:

$$P_L.P_L = (k^i k^j / k^2)(k_i k_j / k^2) = 1, \quad (31)$$

$$P_T.P_T = (\delta^{ij} - k^i k^j / k^2)(\delta_{ij} - k_i k_j / k^2) = 2, \quad (32)$$

$$P_L.P_T = (k^i k^j / k^2).(\delta_{ij} - k_i k_j / k^2) = 0, \quad (33)$$

$$P_L.P_b = (k^i k^j / k^2)(b_i b_j) = 0, \quad (34)$$

$$P_T.P_b = (\delta^{ij} - k^i k^j / k^2)(b_i b_j) = 1, \quad (35)$$

$$P_L.P_{bk} = (k^i k^j / k^2)(\epsilon_{ij\eta} b^\eta) = 0, \quad (36)$$

$$P_T.P_{bk} = (\delta^{ij} - k^i k^j / k^2)(\epsilon_{ij\eta} b^\eta) = 0, \quad (37)$$

$$P_b.P_{bk} = (b^i b^j)(\epsilon_{ij\eta} b^\eta) = 0, \quad (38)$$

$$P_{bk}.P_{bk} = (\epsilon^{ij\eta} b_\eta)(\epsilon_{ij\eta} b^\eta) = 1, \quad (39)$$

where $P_a.P_c = (P_a)^{ij}(P_c)_{ij}$ and the dot product refers to the contraction of both indices. The polarization tensor in Eq. (24) can be written in terms of the projection tensors as

$$\Pi^{ij} = i\omega\sigma_e P_L + i\omega\sigma_e P_T + i\omega\sigma_H P_{bk}. \quad (40)$$

Using the contractions, Eqs. (31)–(39), to find the coefficients of Eq. (30) in terms of Eq. (24),

$$\Pi.P_L = \alpha_0 = i\omega\sigma_e, \qquad \Pi.P_T = 2\beta_0 + \gamma_0 = 2i\omega\sigma_e, \quad (41)$$

$$\Pi.P_b = \gamma_0 + \beta_0 = i\omega\sigma_e, \qquad \Pi.P_{bk} = \delta_0 = i\omega\sigma_H. \quad (42)$$

With these, the coefficients are found to be

$$\begin{aligned} \alpha_0 &= i\omega\sigma_e, & \beta_0 &= i\omega\sigma_e, \\ \gamma_0 &= 0, & \delta_0 &= i\omega\sigma_H. \end{aligned} \quad (43)$$

The structure function corresponding to P_b^{ij} and along the direction of the magnetic fields is shown to be zero, $\gamma_0 = 0$, and the rest, α_0, β_0, and δ_0 are shown to be related to the conductivities.

B. Propagator and the dispersion relation

The inverse of the propagator can be obtained from the relation with the Polarization tensor,

$$[\Delta^{-1}]^{ij} = \alpha_1 P_L^{ij} + \beta_1 P_T^{ij} + \delta_1 P_{bk}^{ij}, \quad (44)$$

where the coefficients are obtained as

$$\alpha_1 = (-\omega^2 + \alpha_0), \quad \beta_1 = [(k^2 - \omega^2) + \beta_0], \quad \delta_1 = \delta_0, \quad (45)$$

where the coefficient γ_1 corresponding to P_b^{ij} is $\gamma_1 = \gamma_0 = 0$.

The tensor exists in the same space as its inverse; hence, we can expand the propagator along the same components and obtain

$$[\Delta]^{ij} = \alpha_2 P_L^{ij} + \beta_2 P_T^{ij} + \delta_2 P_{bk}^{ij}, \quad (46)$$

using the property, $[\Delta^{-1}]^{ij}[\Delta]_{j\eta} = \delta_\eta^i$, and using the following contractions:

$$(P_T)^{ij}(P_T)_{j\eta} = \left[\delta_\eta^i - \frac{k^i k_\eta}{k^2}\right], \quad (47)$$

$$(P_L)^{ij}(P_L)_{j\eta} = \frac{k^i k_\eta}{k^2}, \quad (48)$$

$$(P_T)^{ij}(P_{bk})_{j\eta} = \epsilon_{\eta\theta}^i b^\theta - \frac{k^i k^j}{k^2}\epsilon_{j\eta\theta}b^\theta, \quad (49)$$

$$(P_T)^{ij}(P_L)_{j\eta} = 0, \quad (50)$$

$$(P_L)^{ij}(P_{bk})_{j\eta} = \frac{k^i k^j}{k^2}\epsilon_{j\eta\theta}b^\theta, \quad (51)$$

$$(P_{bk})^{ij}(P_{bk})_{j\eta} = -\delta_\eta^i + b_\eta b^i, \quad (52)$$

we obtain the coefficients of the propagator as

$$\alpha_2 = -\frac{-2\alpha_1\beta_1 - 2\beta_1^2 - \delta_1 2}{(\alpha_1 + \beta_1)(\alpha_1\beta_1 + \delta_1^2)}, \quad (53)$$

$$\beta_2 = -\frac{-\alpha_1^2 - \alpha_1\beta_1 + \delta_1^2}{(\alpha_1 + \beta_1)(\alpha_1\beta_1 + \delta_1^2)}, \quad (54)$$

$$\delta_2 = -\frac{(\alpha_1 + \beta_1)\delta_1}{(\alpha_1 + \beta_1)(\alpha_1\beta_1 + \delta_1^2)}. \quad (55)$$

To find the poles and the dispersion relations, we can solve for the denominators to be zero, which are factorized as

$$\Delta_1 = \alpha_1 + \beta_1 = 0; \qquad \Delta_2 = \alpha_1\beta_1 + \delta_1^2. \quad (56)$$

The dispersion relations of Δ_1 are found by setting $(-2\omega^2 + k^2 + 2i\omega\sigma_e) = 0$,

$$\begin{aligned} \omega_1 &= \frac{i\sigma_e + i\sqrt{(\sigma_e^2 - 2k^2)}}{2}, \\ \omega_2 &= \frac{i\sigma_e - i\sqrt{(\sigma_e^2 - 2k^2)}}{2}. \end{aligned} \quad (57)$$

The dispersion relations of Δ_2 can be found by setting $(-\omega^2 + i\omega\sigma_e)(k^2 - \omega^2 + i\omega\sigma_e) - \omega^2\sigma_H^2 = 0$ and solving for ω,

$$\omega_3 = \frac{2i\omega\sigma_e}{3} - \frac{2^{1/3}[(i\omega\sigma_e)^2 - 3(i\omega\sigma_H)^2 - 3k^2]}{3l} + \frac{l}{3 \times 2^{1/3}}, \quad (58)$$

$$\begin{aligned} \omega_4 &= \frac{2i\omega\sigma_e}{3} + \frac{(1 + i\sqrt{3})[(i\omega\sigma_e)^2 - 3(i\omega\sigma_H)^2 - 3k^2]}{2^{2/3} \times 3l} \\ &\quad - \frac{(1 - i\sqrt{3})l}{6 \times 2^{1/3}}, \end{aligned}$$

$$\begin{aligned} \omega_5 &= \frac{2i\omega\sigma_e}{3} + \frac{(1 - i\sqrt{3})[(i\omega\sigma_e)^2 - 3(i\omega\sigma_H)^2 - 3k^2]}{2^{2/3} \times 3l} \\ &\quad - \frac{(1 + i\sqrt{3})l}{6 \times 2^{1/3}}, \end{aligned} \quad (59)$$

where

$$\begin{aligned} l &= \Big[2i(i\omega\sigma_e)^3 + 18i((i\omega\sigma_e)(i\omega\sigma_h^2)^2) - 9i(i\omega\sigma_e)k^2 \\ &\quad + \big(4[(i\omega\sigma_e)^2 - 3(i\omega\sigma_H)^2 - 3k^2]^3 + 2i(i\omega\sigma_e)^3 \\ &\quad + 18i(i\omega\sigma_e)(i\omega\sigma_H)^2 - 9i(i\omega\sigma_e)k^2]^2\big)^{1/2}\Big]^{1/3} \end{aligned} \quad (60)$$

with $\omega_6 = 0$. The hot QCD medium in the presence of a weak magnetic field shows five modes; among these, only the positive energy dispersion relations are considered. The negative modes can be shown to arise due to the ambiguity

in the positive and negative directions of the orthonormal basis we have constructed.

IV. ENERGY LOSS OF A HEAVY QUARK

A heavy quark moving in the medium loses its energy and is described by Wong's equation. The classical equations which describe the evolution of a point charged particle are given by

$$\frac{dx^\mu(\tau)}{d\tau} = u^\mu(\tau),$$
$$\frac{dp^\mu(\tau)}{d\tau} = gq^a(\tau)F_a^{\mu\nu}(x(\tau))u_\nu(\tau),$$
$$\frac{dq^a(\tau)}{d\tau} = -gf^{abc}u_\mu(\tau)A_b^\mu(x(\tau))q_c(\tau), \qquad (61)$$

where τ, $x(\tau)$, and $p^\mu(\tau)$ are the proper time, the trajectory, and the four momentum of the heavy patron, respectively. The four velocity u^μ is given by $u^\mu = \frac{p^\mu(\tau)}{m}$ with m being the mass of the heavy particle.

The energy loss expression of the heavy patrons is obtained by imposing two conditions on Wong's equation. First, the gauge condition where $u^\mu A_a^\mu = 0$ implies that the third Wong's equation goes to zero, or the charge is independent of the proper time and a constant. The second condition is that the quark's momentum and energy evolve in time without changing the magnitude of its velocity while interacting with the field. Now considering the second Wong's equation, it simplifies under these conditions,

$$-\frac{dE}{dX} = gq^a \frac{\mathbf{u}}{|\mathbf{u}|}.\mathbf{E}_{\text{ind}}^a(X). \qquad (62)$$

The induced field, $E_{\text{ind}}(X)$, can be obtained from the equation of the propagator,

$$E_{\text{ind}}^j(K) = i\omega[\Delta^{ij}(k)]J_i^{\text{ext}}(K). \qquad (63)$$

The external current of a point charge in Fourier space is given by

$$\mathbf{J}_{\text{ext}}(K) = \frac{igq^a\mathbf{u}}{\omega - \mathbf{u}.\mathbf{k} + i0^+}. \qquad (64)$$

Contracting the external current with the propagator, we obtain the induced electric field

$$E_{\text{ind}}^j(X) = -igq \int d\omega d^3\mathbf{k}\left(\alpha_2 P_L^{ij}u_i + \beta_2 P_T^{ij}u_i + \delta_2 P_{bk}^{ij}u_i\right)$$
$$\times \frac{\exp i(k^i x_i - \omega t)}{\omega - u^i.k_i + i0^+}, \qquad (65)$$

and using this, the energy loss of the heavy patron can be written as

$$-\frac{dE}{dX} = \frac{C_F\alpha_s}{2\pi^2|\mathbf{u}|} \int d\omega d^3\mathbf{k}\left(\alpha_2 P_L^{ij}u_iu_j + \beta_2 P_T^{ij}u_iu_j\right.$$
$$\left. + \delta_2 P_{bk}^{ij}u_iu_j\right) \frac{\exp i(k^i x_i - \omega t)}{\omega - u^i.k_i + i0^+}, \qquad (66)$$

with $C_F = 4/3$ being the Casimir invariant and α_s is the QCD coupling constant. It can be seen that the antisymmetric projection tensor does not contribute to the energy loss of heavy quarks due to the projection of u^iu^j being zero, $(P_{bk}^{ij})u^iu^j = 0$.

V. RESULTS AND DISCUSSIONS

The dynamics of the hot QCD matter can be understood through the dispersion relations and can be obtained by solving for ω in Δ_1 and Δ_2 as given in Eq. (56). The solution to Δ_1 has one positive real dispersion relation and two imaginary solutions. The dispersion relations of Δ_1 are related to σ_e, the Ohmic conductivity. We have plotted the positive real dispersion relation of Δ_1 in the left panel of Fig. 1. The dispersion relation has been normalized with the plasma frequency, $\omega_p^{Lo} = m_D^{Lo}/\sqrt{3}$, and plotted
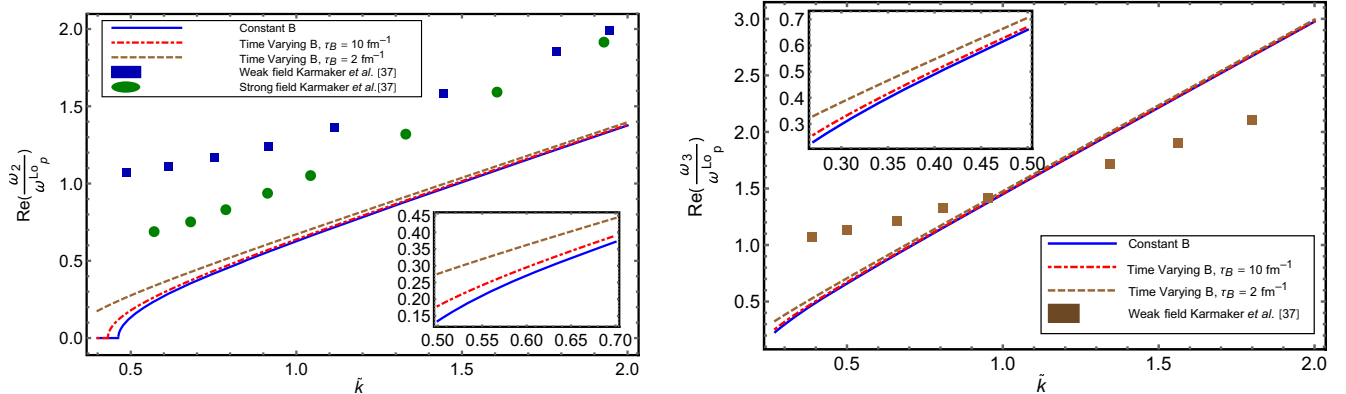

FIG. 1.   Dispersion relation curve of (left panel) ω_2 and (right panel) ω_3 modes with different conditions of the magnetic field, constant magnetic field, and time-varying magnetic field with $\tau_b = 10, 2$ fm^{-1}. The graph is plotted at $T = 2T_C$ with $T_C = 0.17$ GeV.
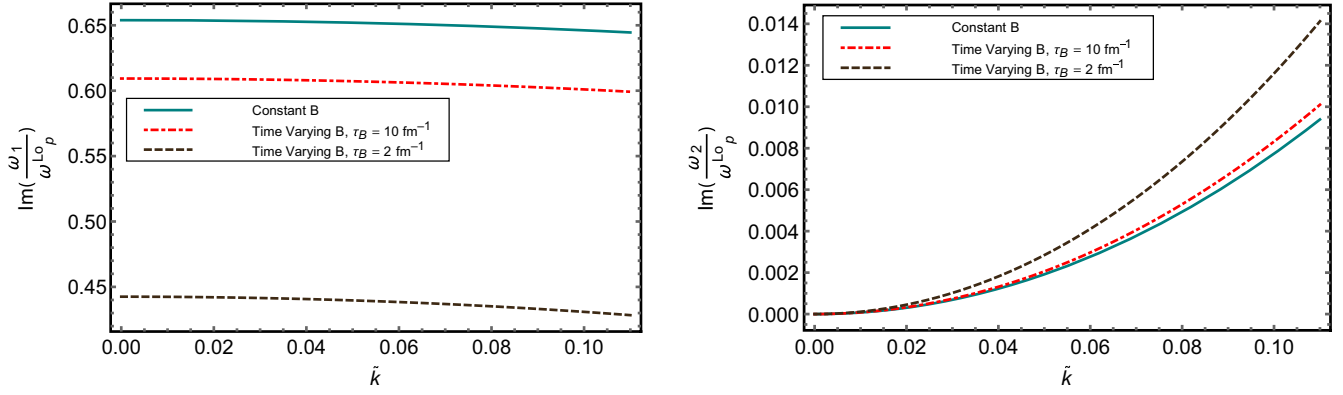
FIG. 2.   Imaginary modes of (left panel) ω_1 and (right panel) ω_2 with different conditions of the magnetic field, constant magnetic field, and time-varying magnetic field with $\tau_b = 10$ fm^{-1} and $\tau_b = 2$ fm^{-1}. The graph is plotted at $T = 2T_C$ with $T_C = 0.17$ GeV.

against $\tilde{k} = k/\omega_p^{Lo}$. The time dependent nature of the magnetic field has been studied by considering three different cases of the magnetic field, constant magnetic field, and time dependent magnetic field with two decay rates of $\tau_b = 10, 2$ fm^{-1}. We see that the effects of the magnetic field are more pronounced in the low $\tilde{k}$ region. The time dependent nature of the magnetic field is seen to increase the dispersion relation with a faster decaying magnetic field, $\tau_b = 2$ fm^{-1}, having the larger effect. The dispersion relation of Δ_2 has one positive real part, ω_3, that has been plotted in the right panel of Fig. 1. The dispersion relation of Δ_2 is related to both the Ohmic and Hall conductivity, with the Hall one related through $\delta_1 = i\omega\sigma_H$. The behavior of ω_3 is similar to that of ω_2 while significantly larger than ω_2.

Our findings have undergone a comparative analysis with the outcomes derived from both weak and strong field hard thermal loop results, as mentioned in [37]. In this work, magnetic fields of magnitudes $|eB| = 0.001$ GeV^2 and $|eB| = 0.36$ GeV^2 were considered for the analysis, with the angles between the magnetic field and the wave number denoted as $\pi/6$ and $\pi/2$, respectively. It is shown in [37] that there are only two positive real modes for the case with the magnetic field being perpendicular to the wave number, $b^i k_i = 0$, as realized in our case, too. It is worth highlighting that the conclusions drawn from the linear response theory align well with those derived from one loop QCD results. To improve the precision of predictions offered by the linear response theory, we propose further refinement through the integration of medium interactions into the distribution function, employing the quasiparticle approach. Another avenue for future investigation would be to analyze the effect of the collision kernels on the dispersion relations by utilizing the Bhatnagar-Gross-Krook collision kernel. However, such considerations are beyond the scope of the present work and are intended to be explored as a future research project.

The imaginary dispersion relations are plotted in Figs. 2–4. The imaginary part of ω_1 is plotted at a constant temperature of $t = 2T_c$ in the left panel of Fig. 2. The time dependent nature of the magnetic field is seen by looking at the three cases of the magnetic field, similar to the analysis in Fig. 1. It is seen to decrease with the normalized wave number, $\tilde{k}$. The time dependent nature of the magnetic field decreases the dispersion relation with a faster decaying magnetic field, $\tau_b = 10$ fm^{-1}, decreasing the dispersion relation the most. In the right panel of Fig. 2, we have plotted the other imaginary dispersion relation in ω_2. The imaginary part of ω_2 increases with $\tilde{k}$, with the faster decaying magnetic field having the most impact on the dispersion relation. The growing positive imaginary mode of ω_2 may lead to instabilities in the medium.

The dispersion relations of Δ_2 consist of three complex solutions. The imaginary parts of ω_3 and ω_4 are plotted in Fig. 3 and the left panel of Fig. 4, respectively. These results underscore the influence of the time dependent magnetic
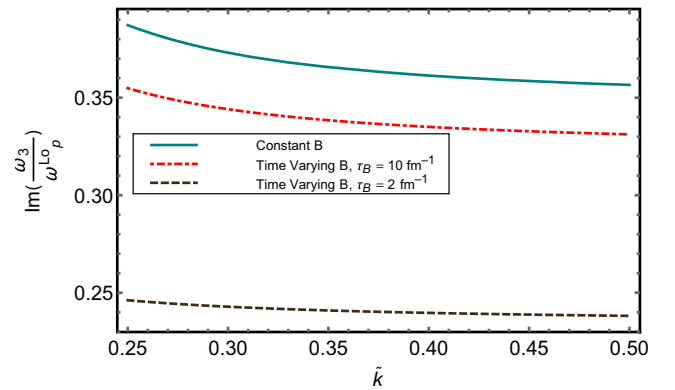

FIG. 3.   Imaginary mode of ω_3 with different conditions of the magnetic field, constant magnetic field, and time-varying magnetic field with $\tau_b = 10$ fm^{-1} and $\tau_b = 2$ fm^{-1}. The graph is plotted at $T = 2T_C$ with $T_C = 0.17$ GeV.
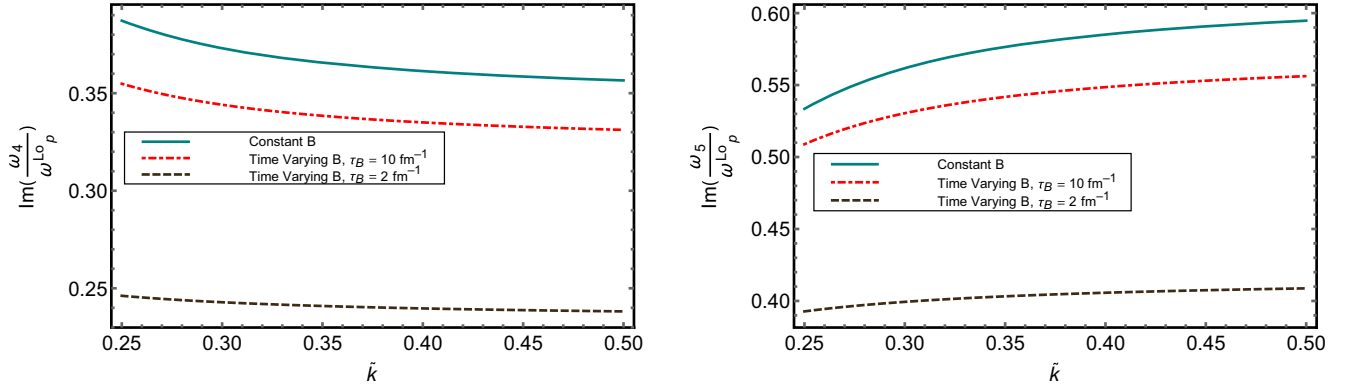
FIG. 4. Imaginary modes of (left panel) ω_4 and (right panel) ω_5 with different conditions of the magnetic field, constant magnetic field, and time-varying magnetic field with $\tau_b = 10$ fm^{-1} and $\tau_b = 2$ fm^{-1}. The graph is plotted at $T = 2T_C$ with $T_C = 0.17$ GeV.
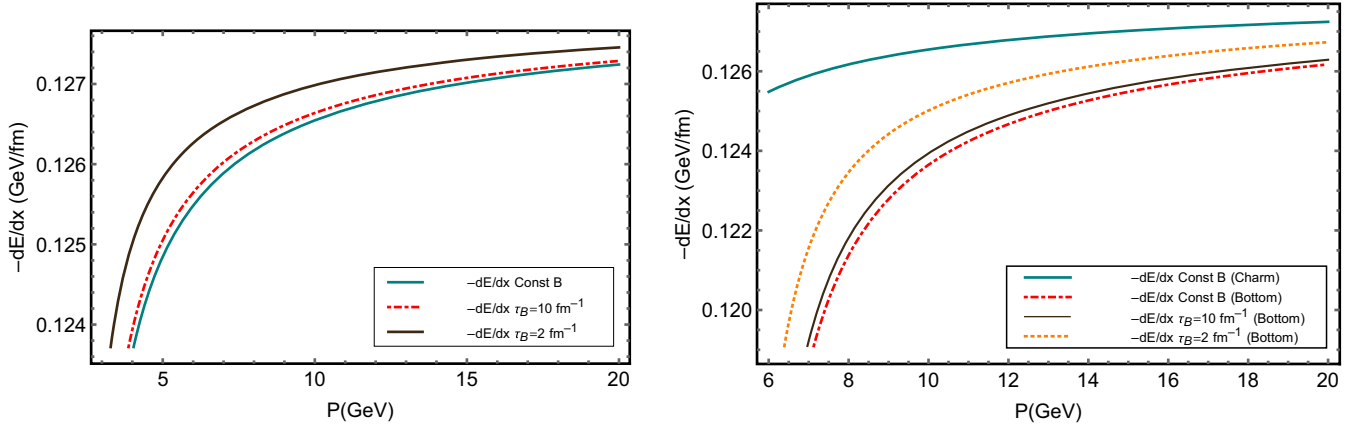

FIG. 5. Energy loss of (left panel) the charm quark and (right panel) the bottom quark, for different conditions of the magnetic field, constant magnetic field, and time-varying magnetic field with $\tau_b = 10$ fm^{-1} and with $\tau_b = 2$ fm^{-1}. The graph is plotted at $T = 2T_C$ with $T_C = 0.17$ GeV.

field, indicating that the decay rate of the magnetic field significantly impacts the dispersion relation. In the right panel of Fig. 4, we have plotted the imaginary part of ω_5. It is seen to be growing with $\tilde{k}$ and may perhaps lead to instabilities in the medium.

The energy loss of heavy quarks is plotted in Fig. 5 for the charm (left panel) and bottom quarks (right panel). The introduction of the time-varying magnetic field increases the energy loss, with a fast decaying magnetic field having the most significant effect. The difference between the energy loss of charm and bottom quarks is also observed and found to be in accordance with an earlier work [44]. The lighter of the two quarks, the charm quark, experiences a greater energy loss within the same momentum range when compared to its heavier counterpart, the bottom quark. This arises due to the fact that a quark with a greater mass travels at a slower velocity when the momentum remains constant. Consequently, a particle moving slowly interacts less with the medium and experiences less energy loss.

VI. CONCLUSION AND OUTLOOK

The collective modes of a hot QCD medium are obtained through the polarization tensor in a background weak time dependent magnetic field within a linear transport theory. The dispersion relation and the collective modes are obtained by invoking Maxwell's equation. The hot QCD medium interactions are incorporated through the collision term in the relaxation time approximation. The dependence of the collective modes on the wave number is plotted, and the effects of the magnetic field are prominent in the lower wave number regions. The imaginary parts of the collective modes are shown to be significantly affected by the magnetic field and are also dependent on the temperature of the medium through the conductivities. We have also observed the energy loss of the heavy quarks moving through a medium in background time dependent electromagnetic fields. The decay rate of the magnetic field is seen to impact the energy loss of the heavy quarks significantly. We observe that the heavier quark (bottom) loses less energy than the lighter (charm) quark, the heavier particle at a fixed value of

momentum p travels at a lower velocity, and a slowly moving particle loses less energy in the medium. These findings are consistent with existing works with constant magnetic fields.

An immediate extension of the work would be to look at the effects of the equation of state on the collective behavior. The effects of momentum anisotropy on the system would also be a good extension of the project. Working with more realistic collision kernels such as the Bhatnagar–Gross–Krook (BGK) and the modified BGK would be another direction where our future investigations will focus. The realization of a hot QCD medium in terms of a refractive index would also be taken up in the future.

Furthermore, investigating R_{AA} in future work could be crucial as it provides a vital link between theoretical predictions and experimental findings.

[1] J. Adams *et al.* (STAR Collaboration), Nucl. Phys. **A757,** 102 (2005).

[2] S. Ryu, J. F. Paquet, C. Shen, G. S. Denicol, B. Schenke, S. Jeon, and C. Gale, Phys. Rev. Lett. **115,** 132301 (2015).

[3] G. Denicol, A. Monnai, and B. Schenke, Phys. Rev. Lett. **116,** 212301 (2016).

[4] S. Acharya *et al.* (ALICE Collaboration), Phys. Rev. Lett. **125,** 022301 (2020).

[5] J. Adam *et al.* (STAR Collaboration), Phys. Rev. Lett. **123,** 162301 (2019).

[6] K. Tuchin, Phys. Rev. C **88,** 024911 (2013).

[7] L. McLerran and V. Skokov, Nucl. Phys. **A929,** 184 (2014).

[8] E. Stewart and K. Tuchin, Nucl. Phys. **A1016,** 122308 (2021).

[9] K. Tuchin, Phys. Rev. C **102,** 014908 (2020).

[10] L. Yan and X.-G. Huang, Phys. Rev. D **107,** 094028 (2023).

[11] B. Feng, Phys. Rev. D **96,** 036009 (2017).

[12] L. Thakur and P. Srivastava, Phys. Rev. D **100,** 076016 (2019).

[13] J. Dey, S. Satapathy, P. Murmu, and S. Ghosh, Pramana **95,** 125 (2021).

[14] K. Hattori, S. Li, D. Satow, and H.-U. Yee, Phys. Rev. D **95,** 076008 (2017).

[15] K. Fukushima and Y. Hidaka, Phys. Rev. Lett. **120,** 162301 (2018).

[16] A. Dash, S. Samanta, J. Dey, U. Gangopadhyaya, S. Ghosh, and V. Roy, Phys. Rev. D **102,** 016016 (2020).

[17] M. Kurian and V. Chandra, Phys. Rev. D **96,** 114026 (2017).

[18] M. Kurian and V. Chandra, Phys. Rev. D **99,** 116018 (2019).

[19] S. Ghosh, A. Bandyopadhyay, R. L. Farias, J. Dey, and G. Krein, Phys. Rev. D **102,** 114015 (2020).

[20] K. K. Gowthama, M. Kurian, and V. Chandra, Phys. Rev. D **103,** 074017 (2021).

[21] G. K. K, M. Kurian, and V. Chandra, Phys. Rev. D **104,** 094037 (2021).

[22] G. S. Denicol, H. Niemi, I. Bouras, E. Molnar, Z. Xu, D. H. Rischke, and C. Greiner, Phys. Rev. D **89,** 074005 (2014).

[23] J. I. Kapusta and J. M. Torres-Rincon, Phys. Rev. C **86,** 054911 (2012).

[24] M. Kurian, Phys. Rev. D **103,** 054024 (2021).

[25] G. K. K, M. Kurian, and V. Chandra, Phys. Rev. D **106,** 034008 (2022).

[26] M. Carrington, T. Fugleberg, D. Pickering, and M. Thoma, Can. J. Phys. **82,** 671 (2004).

[27] B. Schenke, M. Strickland, C. Greiner, and M. H. Thoma, Phys. Rev. D **73,** 125004 (2006).

[28] M. E. Carrington, K. Deja, and S. Mrowczynski, Phys. Rev. C **90,** 034913 (2014).

[29] P. Romatschke and M. Strickland, Phys. Rev. D **68,** 036004 (2003).

[30] P. Romatschke and M. Strickland, Phys. Rev. D **70,** 116006 (2004).

[31] A. Kumar, M. Y. Jamal, V. Chandra, and J. R. Bhatt, Phys. Rev. D **97,** 034007 (2018).

[32] M. Y. Jamal, S. Mitra, and V. Chandra, Phys. Rev. D **95,** 094022 (2017).

[33] V. Skokov, A. Illarionov, and V. Toneev, Int. J. Mod. Phys. A **24,** 5925 (2009).

[34] Y. Zhong, C.-B. Yang, X. Cai, and S.-Q. Feng, Adv. High Energy Phys. **2014,** 193039 (2014).

[35] V. Voronyuk, V. Toneev, W. Cassing, E. Bratkovskaya, V. Konchakovski, and S. Voloshin, Phys. Rev. C **83,** 054911 (2011).

[36] W.-T. Deng and X.-G. Huang, Phys. Rev. C **85,** 044907 (2012).

[37] B. Karmakar, A. Bandyopadhyay, N. Haque, and M. G. Mustafa, Eur. Phys. J. C **79,** 658 (2019).

[38] K. Hattori and D. Satow, Phys. Rev. D **97,** 014023 (2018).

[39] A. Ayala, J. D. Castaño Yepes, L. A. Hernández, J. Salinas San Martín, and R. Zamora, Eur. Phys. J. A **57,** 140 (2021).

[40] A. Ayala, A. Sanchez, G. Piccinelli, and S. Sahu, Phys. Rev. D **71,** 023004 (2005).

[41] M. Formanek, C. Grayson, J. Rafelski, and B. Müller, Ann. Phys. (Amsterdam) **434,** 168605 (2021).

[42] M. Elias, J. Peralta-Ramos, and E. Calzetta, Phys. Rev. D **90,** 014038 (2014).

[43] C. Han, D.-f. Hou, B.-f. Jiang, and J.-r. Li, Eur. Phys. J. A **53,** 205 (2017).

[44] M. Yousuf Jamal and V. Chandra, Eur. Phys. J. C **79,** 761 (2019).

[45] R. Ghosh, M. Y. Jamal, and M. Kurian, Phys. Rev. D **108,** 054035 (2023).

[46] M. Y. Jamal, J. Prakash, I. Nilima, and A. Bandyopadhyay, arXiv:2304.09851.

[47] E. Braaten and M. H. Thoma, Phys. Rev. D **44,** R2625 (1991).

[48] S. Mrowczynski, Phys. Lett. B **269,** 383 (1991).

[49] M. H. Thoma, Phys. Lett. B **273,** 128 (1991).

[50] A. Hosoya and K. Kajantie, Nucl. Phys. **B250,** 666 (1985).

[51] A. Puglisi, S. Plumari, and V. Greco, Phys. Rev. D **90,** 114009 (2014).

[52] M. Hongo, Y. Hirono, and T. Hirano, Phys. Lett. B **775,** 266 (2017).

[53] D. Satow, Phys. Rev. D **90,** 034018 (2014).